Measurement of $\bar{B}^0 \to D^{(*)0}\bar{K}^{(*)0}$ branching fractions

B. Aubert,[1] R. Barate,[1] D. Boutigny,[1] F. Couderc,[1] Y. Karyotakis,[1] J. P. Lees,[1] V. Poireau,[1] V. Tisserand,[1] A. Zghiche,[1] E. Grauges,[2] A. Palano,[3] M. Pappagallo,[3] J. C. Chen,[4] N. D. Qi,[4] G. Rong,[4] P. Wang,[4] Y. S. Zhu,[4] G. Eigen,[5] I. Ofte,[5] B. Stugu,[5] G. S. Abrams,[6] M. Battaglia,[6] D. S. Best,[6] D. N. Brown,[6] J. Button-Shafer,[6] R. N. Cahn,[6] E. Charles,[6] C. T. Day,[6] M. S. Gill,[6] A. V. Gritsan,[6,*] Y. Groysman,[6] R. G. Jacobsen,[6] J. A. Kadyk,[6] L. T. Kerth,[6] Yu. G. Kolomensky,[6] G. Kukartsev,[6] G. Lynch,[6] L. M. Mir,[6] P. J. Oddone,[6] T. J. Orimoto,[6] M. Pripstein,[6] N. A. Roe,[6] M. T. Ronan,[6] W. A. Wenzel,[6] M. Barrett,[7] K. E. Ford,[7] T. J. Harrison,[7] A. J. Hart,[7] C. M. Hawkes,[7] S. E. Morgan,[7] A. T. Watson,[7] M. Fritsch,[8] K. Goetzen,[8] T. Held,[8] H. Koch,[8] B. Lewandowski,[8] M. Pelizaeus,[8] K. Peters,[8] T. Schroeder,[8] M. Steinke,[8] J. T. Boyd,[9] J. P. Burke,[9] W. N. Cottingham,[9] D. Walker,[9] T. Cuhadar-Donszelmann,[10] B. G. Fulsom,[10] C. Hearty,[10] N. S. Knecht,[10] T. S. Mattison,[10] J. A. McKenna,[10] A. Khan,[11] P. Kyberd,[11] M. Saleem,[11] L. Teodorescu,[11] V. E. Blinov,[12] A. D. Bukin,[12] A. Buzykaev,[12] V. P. Druzhinin,[12] V. B. Golubev,[12] A. P. Onuchin,[12] S. I. Serednyakov,[12] Yu. I. Skovpen,[12] E. P. Solodov,[12] K. Yu Todyshev,[12] M. Bondioli,[13] M. Bruinsma,[13] M. Chao,[13] S. Curry,[13] I. Eschrich,[13] D. Kirkby,[13] A. J. Lankford,[13] P. Lund,[13] M. Mandelkern,[13] R. K. Mommsen,[13] W. Roethel,[13] D. P. Stoker,[13] S. Abachi,[14] C. Buchanan,[14] S. D. Foulkes,[15] J. W. Gary,[15] O. Long,[15] B. C. Shen,[15] K. Wang,[15] L. Zhang,[15] D. del Re,[16] H. K. Hadavand,[16] E. J. Hill,[16] H. P. Paar,[16] S. Rahatlou,[16] V. Sharma,[16] J. W. Berryhill,[17] C. Campagnari,[17] A. Cunha,[17] B. Dahmes,[17] T. M. Hong,[17] J. D. Richman,[17] T. W. Beck,[18] A. M. Eisner,[18] C. J. Flacco,[18] C. A. Heusch,[18] J. Kroseberg,[18] W. S. Lockman,[18] G. Nesom,[18] T. Schalk,[18] B. A. Schumm,[18] A. Seiden,[18] P. Spradlin,[18] D. C. Williams,[18] M. G. Wilson,[18] J. Albert,[19] E. Chen,[19] G. P. Dubois-Felsmann,[19] A. Dvoretskii,[19] D. G. Hitlin,[19] I. Narsky,[19] T. Piatenko,[19] F. C. Porter,[19] A. Ryd,[19] A. Samuel,[19] R. Andreassen,[20] G. Mancinelli,[20] B. T. Meadows,[20] M. D. Sokoloff,[20] F. Blanc,[21] P. C. Bloom,[21] S. Chen,[21] W. T. Ford,[21] J. F. Hirschauer,[21] A. Kreisel,[21] U. Nauenberg,[21] A. Olivas,[21] W. O. Ruddick,[21] J. G. Smith,[21] K. A. Ulmer,[21] S. R. Wagner,[21] J. Zhang,[21] A. Chen,[22] E. A. Eckhart,[22] A. Soffer,[22] W. H. Toki,[22] R. J. Wilson,[22] F. Winklmeier,[22] Q. Zeng,[22] D. D. Altenburg,[23] E. Feltresi,[23] A. Hauke,[23] H. Jasper,[23] B. Spaan,[23] T. Brandt,[24] V. Klose,[24] H. M. Lacker,[24] R. Nogowski,[24] A. Petzold,[24] J. Schubert,[24] K. R. Schubert,[24] R. Schwierz,[24] J. E. Sundermann,[24] A. Volk,[24] D. Bernard,[25] G. R. Bonneaud,[25] P. Grenier,[25,†] E. Latour,[25] Ch. Thiebaux,[25] M. Verderi,[25] D. J. Bard,[26] P. J. Clark,[26] W. Gradl,[26] F. Muheim,[26] S. Playfer,[26] Y. Xie,[26] M. Andreotti,[27] D. Bettoni,[27] C. Bozzi,[27] R. Calabrese,[27] G. Cibinetto,[27] E. Luppi,[27] M. Negrini,[27] L. Piemontese,[27] F. Anulli,[28] R. Baldini-Ferroli,[28] A. Calcaterra,[28] R. de Sangro,[28] G. Finocchiaro,[28] S. Pacetti,[28] P. Patteri,[28] I. M. Peruzzi,[28,‡] M. Piccolo,[28] M. Rama,[28] A. Zallo,[28] A. Buzzo,[29] R. Capra,[29] R. Contri,[29] M. Lo Vetere,[29] M. M. Macri,[29] M. R. Monge,[29] S. Passaggio,[29] C. Patrignani,[29] E. Robutti,[29] A. Santroni,[29] S. Tosi,[29] G. Brandenburg,[30] K. S. Chaisanguanthum,[30] M. Morii,[30] J. Wu,[30] R. S. Dubitzky,[31] J. Marks,[31] S. Schenk,[31] U. Uwer,[31] W. Bhimji,[32] D. A. Bowerman,[32] P. D. Dauncey,[32] U. Egede,[32] R. L. Flack,[32] J. R. Gaillard,[32] J. A. Nash,[32] M. B. Nikolich,[32] W. Panduro Vazquez,[32] X. Chai,[33] M. J. Charles,[33] W. F. Mader,[33] U. Mallik,[33] V. Ziegler,[33] J. Cochran,[34] H. B. Crawley,[34] L. Dong,[34] V. Eyges,[34] W. T. Meyer,[34] S. Prell,[34] E. I. Rosenberg,[34] A. E. Rubin,[34] G. Schott,[35] N. Arnaud,[36] M. Davier,[36] G. Grosdidier,[36] A. Höcker,[36] F. Le Diberder,[36] V. Lepeltier,[36] A. M. Lutz,[36] A. Oyanguren,[36] T. C. Petersen,[36] S. Pruvot,[36] S. Rodier,[36] P. Roudeau,[36] M. H. Schune,[36] A. Stocchi,[36] W. F. Wang,[36] G. Wormser,[36] C. H. Cheng,[37] D. J. Lange,[37] D. M. Wright,[37] C. A. Chavez,[38] I. J. Forster,[38] J. R. Fry,[38] E. Gabathuler,[38] R. Gamet,[38] K. A. George,[38] D. E. Hutchcroft,[38] D. J. Payne,[38] K. C. Schofield,[38] C. Touramanis,[38] A. J. Bevan,[39] F. Di Lodovico,[39] W. Menges,[39] R. Sacco,[39] C. L. Brown,[40] G. Cowan,[40] H. U. Flaecher,[40] D. A. Hopkins,[40] P. S. Jackson,[40] T. R. McMahon,[40] S. Ricciardi,[40] F. Salvatore,[40] D. N. Brown,[41] C. L. Davis,[41] J. Allison,[42] N. R. Barlow,[42] R. J. Barlow,[42] Y. M. Chia,[42] C. L. Edgar,[42] M. P. Kelly,[42] G. D. Lafferty,[42] M. T. Naisbit,[42] J. C. Williams,[42] J. I. Yi,[42] C. Chen,[43] W. D. Hulsbergen,[43] A. Jawahery,[43] D. Kovalskyi,[43] C. K. Lae,[43] D. A. Roberts,[43] G. Simi,[43] G. Blaylock,[44] C. Dallapiccola,[44] S. S. Hertzbach,[44] X. Li,[44] T. B. Moore,[44] S. Saremi,[44] H. Staengle,[44] S. Y. Willocq,[44] R. Cowan,[45] K. Koeneke,[45] G. Sciolla,[45] S. J. Sekula,[45] M. Spitznagel,[45] F. Taylor,[45] R. K. Yamamoto,[45] H. Kim,[46] P. M. Patel,[46] C. T. Potter,[46] S. H. Robertson,[46] A. Lazzaro,[47] V. Lombardo,[47] F. Palombo,[47] J. M. Bauer,[48] L. Cremaldi,[48] V. Eschenburg,[48] R. Godang,[48] R. Kroeger,[48] J. Reidy,[48] D. A. Sanders,[48] D. J. Summers,[48] H. W. Zhao,[48] S. Brunet,[49] D. Côté,[49] M. Simard,[49] P. Taras,[49] F. B. Viaud,[49] H. Nicholson,[50] N. Cavallo,[51,§] G. De Nardo,[51] F. Fabozzi,[51,§] C. Gatto,[51] L. Lista,[51] D. Monorchio,[51] P. Paolucci,[51] D. Piccolo,[51] C. Sciacca,[51] M. Baak,[52] H. Bulten,[52] G. Raven,[52] H. L. Snoek,[52] C. P. Jessop,[53] J. M. LoSecco,[53] T. Allmendinger,[54] G. Benelli,[54] K. K. Gan,[54] K. Honscheid,[54] D. Hufnagel,[54] P. D. Jackson,[54] H. Kagan,[54] R. Kass,[54] T. Pulliam,[54] A. M. Rahimi,[54] R. Ter-Antonyan,[54] Q. K. Wong,[54] N. L. Blount,[55] J. Brau,[55] R. Frey,[55] O. Igonkina,[55] M. Lu,[55] R. Rahmat,[55] N. B. Sinev,[55] D. Strom,[55] J. Strube,[55] E. Torrence,[55] F. Galeazzi,[56] A. Gaz,[56] M. Margoni,[56] M. Morandin,[56] A. Pompili,[56] M. Posocco,[56] M. Rotondo,[56]

031101-1

F. Simonetto,[56] R. Stroili,[56] C. Voci,[56] M. Benayoun,[57] J. Chauveau,[57] P. David,[57] L. Del Buono,[57] Ch. de la Vaissière,[57]
O. Hamon,[57] B. L. Hartfiel,[57] M. J. J. John,[57] Ph. Leruste,[57] J. Malclès,[57] J. Ocariz,[57] L. Roos,[57] G. Therin,[57] P. K. Behera,[58]
L. Gladney,[58] J. Panetta,[58] M. Biasini,[59] R. Covarelli,[59] M. Pioppi,[59] C. Angelini,[60] G. Batignani,[60] S. Bettarini,[60]
F. Bucci,[60] G. Calderini,[60] M. Carpinelli,[60] R. Cenci,[60] F. Forti,[60] M. A. Giorgi,[60] A. Lusiani,[60] G. Marchiori,[60]
M. A. Mazur,[60] M. Morganti,[60] N. Neri,[60] E. Paoloni,[60] G. Rizzo,[60] J. Walsh,[60] M. Haire,[61] D. Judd,[61] D. E. Wagoner,[61]
J. Biesiada,[62] N. Danielson,[62] P. Elmer,[62] Y. P. Lau,[62] C. Lu,[62] J. Olsen,[62] A. J. S. Smith,[62] A. V. Telnov,[62] F. Bellini,[63]
G. Cavoto,[63] A. D'Orazio,[63] E. Di Marco,[63] R. Faccini,[63] F. Ferrarotto,[63] F. Ferroni,[63] M. Gaspero,[63] L. Li Gioi,[63]
M. A. Mazzoni,[63] S. Morganti,[63] G. Piredda,[63] F. Polci,[63] F. Safai Tehrani,[63] C. Voena,[63] H. Schröder,[64] R. Waldi,[64]
T. Adye,[65] N. De Groot,[65] B. Franek,[65] E. O. Olaiya,[65] F. F. Wilson,[65] S. Emery,[66] A. Gaidot,[66] S. F. Ganzhur,[66]
G. Hamel de Monchenault,[66] W. Kozanecki,[66] M. Legendre,[66] B. Mayer,[66] G. Vasseur,[66] Ch. Yèche,[66] M. Zito,[66]
W. Park,[67] M. V. Purohit,[67] A. W. Weidemann,[67] J. R. Wilson,[67] M. T. Allen,[68] D. Aston,[68] R. Bartoldus,[68] P. Bechtle,[68]
N. Berger,[68] A. M. Boyarski,[68] R. Claus,[68] J. P. Coleman,[68] M. R. Convery,[68] M. Cristinziani,[68] J. C. Dingfelder,[68]
D. Dong,[68] J. Dorfan,[68] D. Dujmic,[68] W. Dunwoodie,[68] R. C. Field,[68] T. Glanzman,[68] S. J. Gowdy,[68] V. Halyo,[68] C. Hast,[68]
T. Hryn'ova,[68] W. R. Innes,[68] M. H. Kelsey,[68] P. Kim,[68] M. L. Kocian,[68] D. W. G. S. Leith,[68] J. Libby,[68] S. Luitz,[68]
V. Luth,[68] H. L. Lynch,[68] D. B. MacFarlane,[68] H. Marsiske,[68] R. Messner,[68] D. R. Muller,[68] C. P. O'Grady,[68] V. E. Ozcan,[68]
A. Perazzo,[68] M. Perl,[68] B. N. Ratcliff,[68] A. Roodman,[68] A. A. Salnikov,[68] R. H. Schindler,[68] J. Schwiening,[68] A. Snyder,[68]
J. Stelzer,[68] D. Su,[68] M. K. Sullivan,[68] K. Suzuki,[68] S. K. Swain,[68] J. M. Thompson,[68] J. Va'vra,[68] N. van Bakel,[68]
M. Weaver,[68] A. J. R. Weinstein,[68] W. J. Wisniewski,[68] M. Wittgen,[68] D. H. Wright,[68] A. K. Yarritu,[68] K. Yi,[68]
C. C. Young,[68] P. R. Burchat,[69] A. J. Edwards,[69] S. A. Majewski,[69] B. A. Petersen,[69] C. Roat,[69] L. Wilden,[69] S. Ahmed,[70]
M. S. Alam,[70] R. Bula,[70] J. A. Ernst,[70] V. Jain,[70] B. Pan,[70] M. A. Saeed,[70] F. R. Wappler,[70] S. B. Zain,[70] W. Bugg,[71]
M. Krishnamurthy,[71] S. M. Spanier,[71] R. Eckmann,[72] J. L. Ritchie,[72] A. Satpathy,[72] R. F. Schwitters,[72] J. M. Izen,[73]
I. Kitayama,[73] X. C. Lou,[73] S. Ye,[73] F. Bianchi,[74] M. Bona,[74] F. Gallo,[74] D. Gamba,[74] M. Bomben,[75] L. Bosisio,[75]
C. Cartaro,[75] F. Cossutti,[75] G. Della Ricca,[75] S. Dittongo,[75] S. Grancagnolo,[75] L. Lanceri,[75] L. Vitale,[75] V. Azzolini,[76]
F. Martinez-Vidal,[76] R. S. Panvini,[77,||] Sw. Banerjee,[78] B. Bhuyan,[78] C. M. Brown,[78] D. Fortin,[78] K. Hamano,[78]
R. Kowalewski,[78] I. M. Nugent,[78] J. M. Roney,[78] R. J. Sobie,[78] J. J. Back,[79] P. F. Harrison,[79] T. E. Latham,[79]
G. B. Mohanty,[79] H. R. Band,[80] X. Chen,[80] B. Cheng,[80] S. Dasu,[80] M. Datta,[80] A. M. Eichenbaum,[80] K. T. Flood,[80]
M. T. Graham,[80] J. J. Hollar,[80] J. R. Johnson,[80] P. E. Kutter,[80] H. Li,[80] R. Liu,[80] B. Mellado,[80] A. Mihalyi,[80]
A. K. Mohapatra,[80] Y. Pan,[80] M. Pierini,[80] R. Prepost,[80] P. Tan,[80] S. L. Wu,[80] Z. Yu,[80] and H. Neal[81]

[1]*Laboratoire de Physique des Particules, F-74941 Annecy-le-Vieux, France*
[2]*Universitat de Barcelona, Facultat de Fisica Dept. ECM, E-08028 Barcelona, Spain*
[3]*Università di Bari, Dipartimento di Fisica and INFN, I-70126 Bari, Italy*
[4]*Institute of High Energy Physics, Beijing 100039, China*
[5]*University of Bergen, Institute of Physics, N-5007 Bergen, Norway*
[6]*Lawrence Berkeley National Laboratory and University of California, Berkeley, California 94720, USA*
[7]*University of Birmingham, Birmingham, B15 2TT, United Kingdom*
[8]*Ruhr Universität Bochum, Institut für Experimentalphysik 1, D-44780 Bochum, Germany*
[9]*University of Bristol, Bristol BS8 1TL, United Kingdom*
[10]*University of British Columbia, Vancouver, British Columbia, Canada V6T 1Z1*
[11]*Brunel University, Uxbridge, Middlesex UB8 3PH, United Kingdom*
[12]*Budker Institute of Nuclear Physics, Novosibirsk 630090, Russia*
[13]*University of California at Irvine, Irvine, California 92697, USA*
[14]*University of California at Los Angeles, Los Angeles, California 90024, USA*
[15]*University of California at Riverside, Riverside, California 92521, USA*
[16]*University of California at San Diego, La Jolla, California 92093, USA*
[17]*University of California at Santa Barbara, Santa Barbara, California 93106, USA*
[18]*University of California at Santa Cruz, Institute for Particle Physics, Santa Cruz, California 95064, USA*
[19]*California Institute of Technology, Pasadena, California 91125, USA*
[20]*University of Cincinnati, Cincinnati, Ohio 45221, USA*
[21]*University of Colorado, Boulder, Colorado 80309, USA*
[22]*Colorado State University, Fort Collins, Colorado 80523, USA*
[23]*Universität Dortmund, Institut für Physik, D-44221 Dortmund, Germany*
[24]*Technische Universität Dresden, Institut für Kern- und Teilchenphysik, D-01062 Dresden, Germany*
[25]*Ecole Polytechnique, LLR, F-91128 Palaiseau, France*
[26]*University of Edinburgh, Edinburgh EH9 3JZ, United Kingdom*
[27]*Università di Ferrara, Dipartimento di Fisica and INFN, I-44100 Ferrara, Italy*

[28]Laboratori Nazionali di Frascati dell'INFN, I-00044 Frascati, Italy

[29]Università di Genova, Dipartimento di Fisica and INFN, I-16146 Genova, Italy

[30]Harvard University, Cambridge, Massachusetts 02138, USA

[31]Universität Heidelberg, Physikalisches Institut, Philosophenweg 12, D-69120 Heidelberg, Germany

[32]Imperial College London, London, SW7 2AZ, United Kingdom

[33]University of Iowa, Iowa City, Iowa 52242, USA

[34]Iowa State University, Ames, Iowa 50011-3160, USA

[35]Universität Karlsruhe, Institut für Experimentelle Kernphysik, D-76021 Karlsruhe, Germany

[36]Laboratoire de l'Accélérateur Linéaire, IN2P3-CNRS et Université Paris-Sud 11, Centre Scientifique d'Orsay, B.P. 34, F-91898 ORSAY Cedex, France

[37]Lawrence Livermore National Laboratory, Livermore, California 94550, USA

[38]University of Liverpool, Liverpool L69 7ZE, United Kingdom

[39]Queen Mary, University of London, E1 4NS, United Kingdom

[40]University of London, Royal Holloway and Bedford New College, Egham, Surrey TW20 0EX, United Kingdom

[41]University of Louisville, Louisville, Kentucky 40292, USA

[42]University of Manchester, Manchester M13 9PL, United Kingdom

[43]University of Maryland, College Park, Maryland 20742, USA

[44]University of Massachusetts, Amherst, Massachusetts 01003, USA

[45]Massachusetts Institute of Technology, Laboratory for Nuclear Science, Cambridge, Massachusetts 02139, USA

[46]McGill University, Montréal, Québec, Canada H3A 2T8

[47]Università di Milano, Dipartimento di Fisica and INFN, I-20133 Milano, Italy

[48]University of Mississippi, University, Mississippi 38677, USA

[49]Université de Montréal, Physique des Particules, Montréal, Québec, Canada H3C 3J7

[50]Mount Holyoke College, South Hadley, Massachusetts 01075, USA

[51]Università di Napoli Federico II, Dipartimento di Scienze Fisiche and INFN, I-80126, Napoli, Italy

[52]NIKHEF, National Institute for Nuclear Physics and High Energy Physics, NL-1009 DB Amsterdam, The Netherlands

[53]University of Notre Dame, Notre Dame, Indiana 46556, USA

[54]Ohio State University, Columbus, Ohio 43210, USA

[55]University of Oregon, Eugene, Oregon 97403, USA

[56]Università di Padova, Dipartimento di Fisica and INFN, I-35131 Padova, Italy

[57]Universités Paris VI et VII, Laboratoire de Physique Nucléaire et de Hautes Energies, F-75252 Paris, France

[58]University of Pennsylvania, Philadelphia, Pennsylvania 19104, USA

[59]Università di Perugia, Dipartimento di Fisica and INFN, I-06100 Perugia, Italy

[60]Università di Pisa, Dipartimento di Fisica, Scuola Normale Superiore and INFN, I-56127 Pisa, Italy

[61]Prairie View A&M University, Prairie View, Texas 77446, USA

[62]Princeton University, Princeton, New Jersey 08544, USA

[63]Università di Roma La Sapienza, Dipartimento di Fisica and INFN, I-00185 Roma, Italy

[64]Universität Rostock, D-18051 Rostock, Germany

[65]Rutherford Appleton Laboratory, Chilton, Didcot, Oxon, OX11 0QX, United Kingdom

[66]DSM/Dapnia, CEA/Saclay, F-91191 Gif-sur-Yvette, France

[67]University of South Carolina, Columbia, South Carolina 29208, USA

[68]Stanford Linear Accelerator Center, Stanford, California 94309, USA

[69]Stanford University, Stanford, California 94305-4060, USA

[70]State University of New York, Albany, New York 12222, USA

[71]University of Tennessee, Knoxville, Tennessee 37996, USA

[72]University of Texas at Austin, Austin, Texas 78712, USA

[73]University of Texas at Dallas, Richardson, Texas 75083, USA

[74]Università di Torino, Dipartimento di Fisica Sperimentale and INFN, I-10125 Torino, Italy

[75]Università di Trieste, Dipartimento di Fisica and INFN, I-34127 Trieste, Italy

[76]IFIC, Universitat de Valencia-CSIC, E-46071 Valencia, Spain

[77]Vanderbilt University, Nashville, Tennessee 37235, USA

[78]University of Victoria, Victoria, British Columbia, Canada V8W 3P6

[79]Department of Physics, University of Warwick, Coventry CV4 7AL, United Kingdom

---

[*]Also with the Johns Hopkins University, Baltimore, MD 21218, USA

[†]Also at Laboratoire de Physique Corpusculaire, Clermont-Ferrand, France

[‡]Also with Università di Perugia, Dipartimento di Fisica, Perugia, Italy

[§]Also with Università della Basilicata, Potenza, Italy

[‖]Deceased

[80]*University of Wisconsin, Madison, Wisconsin 53706, USA*
[81]*Yale University, New Haven, Connecticut 06511, USA*

We present a study of the decays $\bar{B}^0 \to D^{(*)0}\bar{K}^{(*)0}$ using a sample of 226×10^6 $\Upsilon(4S) \to B\bar{B}$ decays collected with the *BABAR* detector at the PEP-II asymmetric-energy e^+e^- collider at SLAC. We report evidence for the decay of B^0 and $\bar{B}^0$ mesons to the $D^{*0}K_S^0$ final state with an average branching fraction $\mathcal{B}(\tilde{B}^0 \to D^{*0}\tilde{K}^0) \equiv (\mathcal{B}(\bar{B}^0 \to D^{*0}\bar{K}^0) + \mathcal{B}(B^0 \to D^{*0}K^0))/2 = (3.6 \pm 1.2 \pm 0.3) \times 10^{-5}$. Similarly, we measure $\mathcal{B}(\tilde{B}^0 \to D^0\tilde{K}^0) \equiv (\mathcal{B}(\bar{B}^0 \to D^0\bar{K}^0) + \mathcal{B}(B^0 \to D^0K^0))/2 = (5.3 \pm 0.7 \pm 0.3) \times 10^{-5}$ for the $D^0K_S^0$ final state. We measure $\mathcal{B}(\bar{B}^0 \to D^0\bar{K}^{*0}) = (4.0 \pm 0.7 \pm 0.3) \times 10^{-5}$ and set a 90% confidence level upper limit $\mathcal{B}(\bar{B}^0 \to \bar{D}^0\bar{K}^{*0}) < 1.1 \times 10^{-5}$. We determine the upper limit for the decay amplitude ratio $|\mathcal{A}(\bar{B}^0 \to \bar{D}^0\bar{K}^{*0})/\mathcal{A}(\bar{B}^0 \to D^0\bar{K}^{*0})|$ to be less than 0.4 at the 90% confidence level.

With the discovery of *CP* violation in the decays of neutral *B* mesons [1] and the precise measurement [2] of the angle β of the Cabibbo-Kobayashi-Maskawa (CKM) Unitarity Triangle [3], the experimental focus has shifted towards over-constraining the unitarity triangle through precise measurements of $|V_{ub}|$ and the angles α and γ. The angle γ is $\arg(-V_{ub}^*V_{ud}/V_{cb}^*V_{cd})$ and V_{ij} are CKM matrix elements. Several methods have been suggested and explored to measure γ with small uncertainties [4], but they all require large samples of *B* mesons not yet available. The decay modes $\bar{B}^0 \to D^{(*)0}\bar{K}^0$ offer a new approach for the determination of $\sin(2\beta + \gamma)$ from the measurement of time-dependent *CP* asymmetries in these decays [5]. The *CP* asymmetry appears as a result of the interference between two diagrams leading to the same final state $D^{(*)0}K_S^0$ (Fig. 1). A $\bar{B}^0$ meson can either decay via a $b \to c$ quark transition to the $D^{(*)0}\bar{K}^0$ ($\bar{K}^0 \to K_S^0$) final state, or oscillate into a B^0 which then decays via a $\bar{b} \to \bar{u}$ transition to the $D^{(*)0}K^0$ ($K^0 \to K_S^0$) final state [6]. The $\bar{B}^0B^0$ oscillation provides the weak phase 2β and the relative weak phase between the two decay diagrams is γ.

The sensitivity of this method [5] depends on the rates for these decays and the ratio of the decay amplitudes. The branching fractions $\mathcal{B}(\bar{B}^0 \to D^{(*)0}\bar{K}^{(*)0})$ can be estimated from the measured color-suppressed decays $\bar{B}^0 \to D^{(*)0}\pi^0$ [7] to be approximately $\mathcal{B}(\bar{B}^0 \to D^{(*)0}\bar{K}^{(*)0}) \approx \sin^2\theta_c \mathcal{B}(\bar{B}^0 \to D^{(*)0}\pi^0) \sim \mathcal{O}(10^{-5})$, where θ_c is the Cabibbo angle and $\sin\theta_c = 0.22$. The Belle Collaboration has observed the $\bar{B}^0 \to D^0\bar{K}^{(*)0}$ decays with branching fractions consistent with this naive expectation [8]. The time-dependent *CP* asymmetries in $\bar{B}^0 \to D^{(*)0}\bar{K}^0$

decays are proportional to $r_B^{(*)} \cdot \sin(2\beta + \gamma \pm \delta)/(1 + r_B^{(*)2})$, where $r_B^{(*)} \equiv |\mathcal{A}(\bar{B}^0 \to \bar{D}^{(*)0}\bar{K}^0)/\mathcal{A}(\bar{B}^0 \to D^{(*)0}\bar{K}^0)|$ and δ is a relative strong phase which depends on the specific final state. Higher values of $r_B^{(*)}$ lead to larger interference between the $b \to c$ and $b \to u$ processes and thus increased sensitivity to the angle γ. In the standard model $r_B^{(*)} = f \cdot |V_{ub}V_{cs}^*|/|V_{cb}V_{us}^*|$, where the factor f accounts for the difference in the strong interaction dynamics between the $b \to c$ and $b \to u$ processes. There are no theoretical calculations or experimental constraints on f.

In $\bar{B}^0 \to D^{(*)0}\bar{K}^0$ ($\bar{K}^0 \to K_S^0$) decays the strangeness content of the $\bar{K}^0$ is hidden and one cannot distinguish between $\bar{B}^0 \to D^{(*)0}\bar{K}^0$ and $B^0 \to D^{(*)0}K^0$. Therefore a direct determination of $r_B^{(*)}$ from the measured rates is not feasible. In the remainder of this paper we refer to these decays as $\tilde{B}^0 \to D^{(*)0}\tilde{K}^0$. Insight into the *B* decay dynamics affecting $r_B^{(*)}$ can be gained by measuring a similar amplitude ratio $\tilde{r}_B \equiv |\mathcal{A}(\bar{B}^0 \to \bar{D}^0\bar{K}^{*0})/\mathcal{A}(\bar{B}^0 \to D^0\bar{K}^{*0})|$ using the self-tagging decay $\bar{K}^{*0} \to K^-\pi^+$. The $\bar{B}^0 \to D^0\bar{K}^{*0}$ and $\bar{B}^0 \to \bar{D}^0\bar{K}^{*0}$ decays are distinguished by the correlation between the charges of the kaons produced in the decays of the neutral *D* and the $\bar{K}^{*0}$. In the former decay the two kaons in the final state must have the same charge, while in the latter they are oppositely charged. This charge correlation in the final state is diluted by the presence of the doubly-Cabibbo-suppressed decays $D^0 \to K^+\pi^-, K^+\pi^-\pi^0$, and $K^+\pi^-\pi^+\pi^-$. The ratio $\tilde{r}_B$ is related to the experimental observables $\mathcal{R}_i$ defined as

$$\mathcal{R}_i = \frac{\Gamma(\bar{B}^0 \to (K^+X_i^-)_D\bar{K}^{*0})}{\Gamma(\bar{B}^0 \to (K^-X_i^+)_D\bar{K}^{*0})}$$
$$= \tilde{r}_B^2 + r_{D_i}^2 + 2\tilde{r}_B r_{D_i}\cos(\gamma + \delta_i), \qquad (1)$$

where

$$X_i^{\pm} = \pi^{\pm}, \pi^{\pm}\pi^0, \pi^{\pm}\pi^-\pi^+, \qquad (2)$$

$$r_{D_i} = \frac{|\mathcal{A}(D^0 \to K^+X_i^-)|}{|\mathcal{A}(D^0 \to K^-X_i^+)|}, \qquad (3)$$
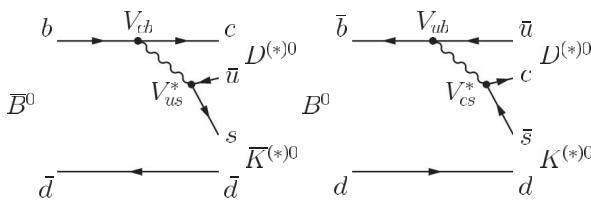
FIG. 1. The decay diagrams for the $b \to c$ transition $\bar{B}^0 \to D^{(*)0}\bar{K}^{(*)0}$ and the $\bar{b} \to \bar{u}$ transition $B^0 \to D^{(*)0}K^{(*)0}$.

$$\delta_i = \delta_B + \delta_{D_i}, \tag{4}$$

and δ_B and δ_{D_i} are strong phase differences between the two B and D_i decay amplitudes, respectively. The values of r_{D_i} have been measured to be $r_{D \to K\pi} = 0.060 \pm 0.002$, $r_{D \to K\pi\pi^0} = 0.066 \pm 0.010$, and $r_{D \to K\pi\pi\pi} = 0.065 \pm 0.010$ [9].

We present herein measurements of the branching fractions $\mathcal{B}(\bar{B}^0 \to D^0\tilde{K}^0)$ and $\mathcal{B}(\bar{B}^0 \to D^0\bar{K}^{*0})$, evidence for the decay $\bar{B}^0 \to D^{*0}\tilde{K}^0$, a 90% confidence level (C.L.) upper limit for the branching fraction of the $b \to u$ transition $\bar{B}^0 \to \bar{D}^0\bar{K}^{*0}$, and a limit for the ratio $\tilde{r}_B$.

These results are based on a sample of 226×10^6 $\Upsilon(4S) \to B\bar{B}$ decays collected with the *BABAR* detector between 1999 and 2004 at the PEP-II asymmetric-energy e^+e^- collider operating at the $\Upsilon(4S)$ resonance. The properties of the continuum $e^+e^- \to q\bar{q}(q = u, d, s, c)$ background events are studied with a data sample of 11.9 fb^{-1} recorded at an energy 40 MeV below the $\Upsilon(4S)$ resonance. The *BABAR* detector has been described in detail elsewhere [10]. Detector components relevant for this analysis are summarized here. Trajectories of charged particles are measured in a spectrometer consisting of a five-layer silicon vertex tracker (SVT) and a 40-layer drift chamber (DCH) operating in a 1.5 T axial magnetic field. Charged particles are identified as pions or kaons using information from a detector of internally reflected Cherenkov light, as well as measurements of energy loss from ionization (dE/dx) in the SVT and the DCH. Photons are detected using an electromagnetic calorimeter composed of 6580 thallium-doped CsI crystals. We use a Monte Carlo simulation of the *BABAR* detector based on GEANT4 [11] to validate the analysis procedure and to study the backgrounds. Simulated events are generated with the EvtGen [12] event generator.

We reconstruct the decays $\bar{B}^0 \to D^0\bar{K}^0, D^{*0}\bar{K}^0, D^0\bar{K}^{*0}$, and $\bar{D}^0\bar{K}^{*0}$ in the decay chains: $D^{*0} \to D^0\pi^0$; $D^0 \to K^-\pi^+$, $K^-\pi^+\pi^0$, and $K^-\pi^+\pi^-\pi^+$; $\bar{K}^0 \to K_S^0 \to \pi^+\pi^-$; $\bar{K}^{*0} \to K^-\pi^+$; and $\pi^0 \to \gamma\gamma$. For each B decay channel the optimal selection criteria are determined by maximizing the ratio $N_S/\sqrt{N_S + N_B}$, where N_S and N_B are, respectively, the expected signal and background yields estimated from samples of simulated events. A large sample of the more abundant $B^+ \to \bar{D}^0\pi^+$ decays, in which the $\bar{D}^0$ decays to the $K^+\pi^-$, $K^+\pi^-\pi^0$, or $K^+\pi^-\pi^+\pi^-$ final states, is used as a calibration sample to measure efficiencies and experimental resolutions for the selection variables.

Well reconstructed charged tracks are used to reconstruct D^0 and K^{*0} candidates. The $K^\pm$ candidates must satisfy a set of kaon identification criteria. These identification criteria have an average efficiency of about 90%, while the probability of a pion to be misidentified as a kaon varies between a few percent and 15%. Photons are reconstructed from energy deposition clusters in the electromagnetic calorimeter consistent with photon showers, and are

required to have an energy greater than 30 MeV. We select π^0 candidates from pairs of photon candidates by requiring their invariant mass to be in the interval 115 MeV/$c^2 < m(\gamma\gamma) < 150$ MeV/c^2.

The K_S^0 candidates are selected from pairs of oppositely charged tracks with invariant mass within 7 MeV/c^2 ($\sim 2\sigma$) of the nominal K_S^0 mass. The displacement of the K_S^0 decay vertex from the interaction point, in the plane perpendicular to the beam axis, divided by its estimated uncertainty must be greater than 2. The K^{*0} candidates are selected from pairs of oppositely charged K^+ and π^- tracks, with invariant mass within 50 MeV/c^2 of the nominal K^{*0} mass. The polarization of the K^{*0} in the B^0 decay is used to reject backgrounds by requiring $|\cos\theta_h| > 0.4$, where the helicity angle θ_h is defined as the angle between the direction of the K^{*0} in the B^0 meson rest frame and the direction of its daughter K^+ in the K^{*0} rest frame. For $\bar{B}^0 \to D^0\bar{K}^{*0}$ and $\bar{B}^0 \to \bar{D}^0\bar{K}^{*0}$ signal candidates, θ_h follows a $\cos^2\theta_h$ distribution, while the combinatorial background is distributed uniformly.

We reconstruct D^0 candidates in the $K^-\pi^+$ and $K^-\pi^+\pi^-\pi^+$ decay modes by combining charged tracks, retaining combinations with an invariant mass within 2σ of the nominal D^0 mass m_{D^0}. In the $D^0 \to K^-\pi^+\pi^0$ selection, the π^0 candidates are required to have a center-of-mass (CM) momentum $p^*_{\pi^0}$ greater than 400 MeV/c. For each $K^-\pi^+\pi^0$ combination, we use the kinematics of the decay products and the known properties of the Dalitz plot for this decay [13] to compute the square of the decay amplitude $\mathcal{A}^2$. We select combinations with $\mathcal{A}^2$ greater than 5% of its maximum value. This requirement selects mostly the $K^-\rho^+$ region of the Dalitz plot. It rejects 62% of the combinatorial background, while keeping 76% of $D^0 \to K^-\pi^+\pi^0$ signal, as measured with the $B^+ \to \bar{D}^0\pi^+$ sample. Combinations with invariant mass within 25 MeV/c^2 (2.5σ) of m_{D^0} are retained.

The D^{*0} candidates are selected from combinations of a D^0 and a π^0 with $p^*_{\pi^0} > 70$ MeV/c. After kinematically constraining D^0 and π^0 candidates to their nominal masses, we select the candidates with a mass difference $\Delta m \equiv |m(D^{*0}) - m(D^0) - 142.2$ MeV/$c^2| < 3.3$ MeV/c^2 (3σ).

Two standard kinematic variables are used to select B^0 candidates: the energy-substituted mass $m_{\text{ES}}c^2 \equiv \sqrt{(\frac{1}{2}s + c^2\mathbf{p}_\Upsilon \cdot \mathbf{p}_B)^2/E_\Upsilon^2 - c^2\mathbf{p}_B^2}$ and the energy difference $\Delta E \equiv E_B^* - \frac{1}{2}\sqrt{s}$, where the asterisk denotes the CM frame, s is the square of the total energy in the CM frame, $\mathbf{p}$ and E are, respectively, three-momentum and energy, and the subscripts Υ and B refer to $\Upsilon(4S)$ and B^0. In calculating $\mathbf{p}_B$ and E_B^* we constrain the mass of the $D^{(*)0}$ and K_S^0 candidates to their respective nominal values. For signal events, m_{ES} is centered around the B^0 mass with a resolution of about 2.6 MeV/c^2, dominated by knowledge of the e^+ and e^- beam energies. In simulated events the

ΔE resolution is found to be ≈ 13 MeV for all B^0 decay modes considered in this analysis. The B^0 candidates are required to have $m_{ES} > 5.2$ GeV/c^2 and $|\Delta E| < 100$ MeV.

We use two variables to reject most of the remaining background, which is dominated by continuum events: a Fisher discriminant [14] based on the energy flow in the event and the polar angle θ_B^* of the B^0 candidate in the CM frame. For correctly reconstructed B candidates $\cos\theta_B^*$ follows a $1 - \cos^2\theta_B^*$ distribution, whereas it is uniformly distributed for continuum events and combinatorial background. We require $|\cos\theta_B^*| < 0.75$ for $\bar{B}^0 \to \bar{D}^0\bar{K}^{*0}$, and $|\cos\theta_B^*| < 0.85$ for all other decay modes. The Fisher discriminant $\mathcal{F}$ is defined as a linear combination of $|\cos\theta_{TB}^*|$ and two energy-flow moments $\mathcal{L}^0$ and $\mathcal{L}^2$. The variable θ_{TB}^* is the angle in the CM frame between the thrust axis [15] of the decay products of the B^0 and the thrust axis of all charged and neutral particles in the event excluding the ones that form the B^0. The energy-flow moments $\mathcal{L}^0$ and $\mathcal{L}^2$ are defined as $\mathcal{L}^i \equiv \sum_j p_j^* \cos^i\theta_j$ where p_j^* is the CM momentum and θ_j is the angle between the direction of particle j with respect to the thrust axis of the B^0 candidate, and the sum is over all particles in the event (excluding those that form the B^0). The requirement on $\mathcal{F}$ varies for each decay channel because of different levels of expected background. In the $D^{(*)0}K_S^0$ and $D^0\bar{K}^{*0}$ final states our requirement has an efficiency of about 80% for the signal while rejecting approximately 85% of the background; in the $\bar{B}^0 \to \bar{D}^0\bar{K}^{*0}$ mode a tighter requirement rejects 95% of the background and has a signal efficiency of 55%.

In the $D^{*0}K_S^0$ final state, approximately 5% of the events that satisfy all selection criteria contain more than one B^0 candidate. We retain the candidate with the smallest χ^2 computed from the measured value of $m(D^0)$ and $m(D^{*0}) - m(D^0)$, their nominal values, and their resolutions in data. In the $D^0K_S^0$, $D^0\bar{K}^{*0}$, and $\bar{D}^0\bar{K}^{*0}$ final states we retain all selected B^0 candidates since the fraction of events with two or more candidates is negligible ($< 1\%$).

The selected $\bar{B}^0 \to D^{(*)0}\bar{K}^{(*)0}$ candidates include small contributions from numbers of B decays to similar final states which are misreconstructed as signal candidates. We have studied these backgrounds with large samples of simulated events, corresponding to between 100 and 1000 times the size of our data sample, for the following categories of decays: (1) $\bar{B}^0 \to D^0\rho^0$, $\rho^0 \to \pi^+\pi^-$ decays, where one of the two pions is misidentified as a charged kaon; (2) $\bar{B}^0 \to D^+\pi^-$ decays followed by Cabibbo-suppressed decays $D^+ \to \bar{K}^{(*)0}K^+$, $\bar{K}^{(*)0}K^+\pi^0$, and $\bar{K}^{(*)0}K^+\pi^-\pi^+$, and $\bar{B}^0 \to D^+K^-$ followed by $D^+ \to \bar{K}^{(*)0}\pi^+$, $\bar{K}^{(*)0}\pi^+\pi^0$, and $\bar{K}^{(*)0}\pi^+\pi^-\pi^0$ reconstructed, respectively, in the $D^0(K^-\pi^+)K^{(*)0}$, $D^0(K^-\pi^+\pi^0)K^{(*)0}$, and $D^0(K^-\pi^+\pi^-\pi^+)K^{(*)0}$ final states; (3) charmless $\bar{B}^0 \to K^-\pi^+K_S^0(n\pi)$ where the K^- and π^+ are wrongly

combined to form a $D^0 \to K^-\pi^+$ candidate; (4) $\bar{B}^0 \to \bar{D}^{*0}K^{(*)0}$, $\bar{D}^{*0} \to \bar{D}^0\gamma$ candidates, where a low-energy photon is not reconstructed; (5) the decays $B^- \to D^{*0}K^-$, $D^{*0} \to D^0\pi^0/\gamma$, $B^- \to D^0K^{*-}$, $K^{*-} \to K^-\pi^0$, $K_S^0\pi^-$, and $B^0 \to D^{*-}K^+$, $D^{*-} \to \bar{D}^0\pi^-$, where a low-energy π^0, π^-, or photon is replaced by a random low-momentum charged particle. The contribution of category (1) is found to be less than 0.01 events and hence is neglected. The contribution of category (2) is also negligible in all modes, except for $B \to D^0\bar{K}^0$, $D^0 \to K^-\pi^+$. We eliminate 87% of these background events by requiring the invariant masses $m(K_S^0K^+)$ and $m(K_S^0\pi^+)$ to be more than 20 MeV/c^2 away from the nominal D^+ mass. The m_{ES} spectrum of the remaining background events in this category, and in categories (3)–(5), show a broad enhancement near the B mass. However, due to the D^0 mass constraint, B^0 candidates with a misreconstructed D^0 do not peak, unlike the signal, in the ΔE distribution at zero. In the decay $\bar{B}^0 \to \bar{D}^0\bar{K}^{*0}$, the charge correlation used in the selection removes all contributions from known B decays included in simulated events.

The signal yield for each B^0 decay mode is determined with a two-dimensional extended unbinned maximum likelihood fit to the m_{ES} and ΔE distributions, separately for each D^0 decay mode. The probability density function (PDF) is a sum of three components: a signal component $\mathcal{G}(m_{ES}) \times \mathcal{G}(\Delta E)$, a background component $\mathcal{G}(m_{ES}) \times \mathcal{P}_1(\Delta E)$, accounting for other B decays misreconstructed as signal, and a combinatorial background component $\mathcal{T}(m_{ES}) \times \mathcal{P}_2(\Delta E)$. Here, $\mathcal{G}(m_{ES})$ is a Gaussian describing the m_{ES} distribution of signal and misreconstructed B decays; $\mathcal{G}(\Delta E)$ is a Gaussian describing the signal ΔE distribution; $\mathcal{P}_i(\Delta E)$ are first-order polynomials describing the ΔE distributions of background events. The m_{ES} distribution of the combinatorial background is parameterized by a threshold function $\mathcal{T}(m_{ES})$ defined as $\mathcal{T}(m_{ES}) \sim m_{ES}\sqrt{1-x^2}\exp\{-\xi(1-x^2)\}$ [16], where $x = 2m_{ES}c^2/\sqrt{s}$ and ξ is a shape parameter. The mean and the resolution of $\mathcal{G}(m_{ES})$ and $\mathcal{G}(\Delta E)$ are fixed to values measured in the $B^+ \to \bar{D}^0\pi^+$ calibration sample.

TABLE I. Signal yield N_S, signal significance $\mathcal{S}$, effective signal efficiency ε_{eff}, and the measured branching fraction $\mathcal{B}$ for the $\tilde{B}^0 \to D^{(*)0}\tilde{K}^0$, $\bar{B}^0 \to D^0\bar{K}^{*0}$, and $\bar{B}^0 \to \bar{D}^0\bar{K}^{*0}$ decays. The efficiency ε_{eff} is defined as $\sum_i \varepsilon_i \times \mathcal{B}_i$, where the sum is over the D^0 decay modes, ε_i are the signal reconstruction efficiencies, and $\mathcal{B}_i$ are the corresponding intermediate branching fractions for D^{*0}, D^0, K^{*0}, and K^0 decays to final states reconstructed in this analysis.

B Mode	N_S	$\mathcal{S}$	ε_{eff} [%]	$\mathcal{B}[10^{-5}]$
$\tilde{B}^0 \to D^0\tilde{K}^0$	104 ± 14	9.2σ	0.82	$5.3 \pm 0.7 \pm 0.3$
$\tilde{B}^0 \to D^{*0}\tilde{K}^0$	17.1 ± 5.2	4.3σ	0.17	$3.6 \pm 1.2 \pm 0.3$
$\bar{B}^0 \to D^0\bar{K}^{*0}$	77 ± 12	7.9σ	0.84	$4.0 \pm 0.7 \pm 0.3$
$\bar{B}^0 \to \bar{D}^0\bar{K}^{*0}$	$-3.6^{+6.8}_{-5.5}$	—	0.47	$0.0 \pm 0.5 \pm 0.3$
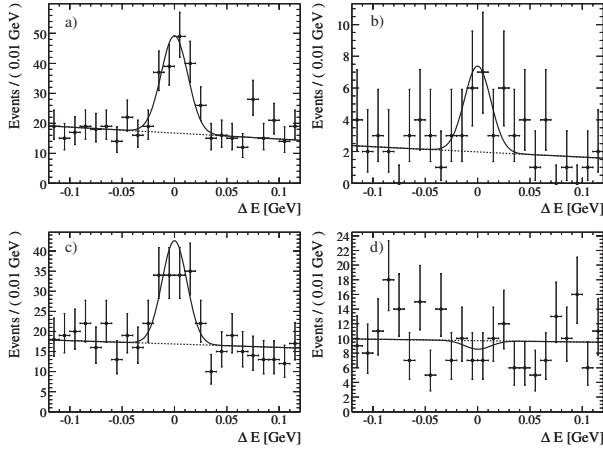
FIG. 2. Distribution of ΔE for a) $\tilde{B}^0 \to D^0\tilde{K}^0$, b) $\tilde{B}^0 \to D^{*0}\tilde{K}^0$, c) $\bar{B}^0 \to D^0\bar{K}^{*0}$, and d) $\bar{B}^0 \to \bar{D}^0\bar{K}^{*0}$ candidates with $|m_{\mathrm{ES}} - 5280\ \mathrm{MeV}/c^2| < 8\ \mathrm{MeV}/c^2$. The points are the data, the solid curve is the projection of the likelihood fit, and the dashed curve represents the background component.

The measured signal yields are summarized in Table I. The ΔE distributions of candidates with $|m_{\mathrm{ES}} - 5280| < 8\ \mathrm{MeV}/c^2$ for the sums of the reconstructed D^0 decay modes are illustrated in Fig. 2. The signal significance $\mathcal{S}$ is computed as $\mathcal{S} = \sqrt{2(\ln\mathcal{L}(N_S) - \ln\mathcal{L}(N_S = 0))}$, where $\mathcal{L}(N_S)$ is the likelihood of the nominal fit, and $\mathcal{L}(N_S = 0)$ is the value obtained after repeating the fit with the signal yield N_S constrained to be zero.

The branching fraction $\mathcal{B}$ for each B^0 decay mode is the weighted average of the branching fractions $\mathcal{B}_j$ in each D^0 channel $D_j = \{K^-\pi^+, K^-\pi^+\pi^-\pi^+, K^-\pi^+\pi^0\}$, computed as

$$\mathcal{B}_j = \frac{N_{S_j}}{2 \times N_{B\bar{B}} \times \mathcal{B}(\Upsilon(4S) \to B^0\bar{B}^0) \times \mathcal{B}_{D_j} \times \mathcal{B}_K \times \varepsilon_j} \tag{5}$$

where N_{S_j} is the signal yield from the likelihood fit, $N_{B\bar{B}}$ is the total number of $\Upsilon(4S) \to B\bar{B}$ events, $\mathcal{B}_{D_j}$ is the branching fraction $\mathcal{B}(D^0 \to D_j)$ in $\tilde{B}^0 \to D^0\tilde{K}^{(*)0}$ and $\mathcal{B}(D^{*0} \to D^0\pi^0) \times \mathcal{B}(D^0 \to D_j)$ in $\tilde{B}^0 \to D^{*0}\tilde{K}^0$, $\mathcal{B}_K$ is the $K^0 \to K_S^0 \to \pi^+\pi^- (K^{*0} \to K^+\pi^-)$ branching fraction in $\tilde{B}^0 \to D^{(*)0}\tilde{K}^0(\bar{B}^0 \to D^0\bar{K}^{*0}, \bar{D}^0\bar{K}^{*0})$, and ε_j is the signal reconstruction efficiency. The weights are calculated from the statistical and uncorrelated systematic uncertainties in $\mathcal{B}_j$. We assume $\mathcal{B}(\Upsilon(4S) \to B^0\bar{B}^0) = 0.5$. The systematic uncertainties for the branching fractions include contributions from estimated misreconstructed B background (1–13%) [17], variation of parameters kept fixed in the likelihood fit (2–8%), $D^{(*)0}$ branching fraction (2.4–6.9%), π^0 reconstruction efficiency (3%), photon reconstruction efficiency (1.8%), charged-track reconstruction efficiency (0.8% per track), simulation statistics (1–4%), efficiency correction factors (1–4%), kaon identification efficiency

(2% per kaon), K_S^0 reconstruction efficiency (1.6%), and the number of $B\bar{B}$ events (1.1%). The efficiency correction factors are obtained by comparing data with MC simulation in the $B^+ \to \bar{D}^0\pi^+$ control sample. The largest contributions to the uncertainties in these factors are from selection requirements for the π^0 momentum $p_{\pi^0}^*$ and the amplitude $|\mathcal{A}|^2$ in the $D^0 \to K^-\pi^+\pi^0$ decay and the Fisher discriminant $\mathcal{F}$. We measure

$$\mathcal{B}(\tilde{B}^0 \to D^0\tilde{K}^0) = (5.3 \pm 0.7 \pm 0.3) \times 10^{-5}$$
$$\mathcal{B}(\tilde{B}^0 \to D^{*0}\tilde{K}^0) = (3.6 \pm 1.2 \pm 0.3) \times 10^{-5}$$
$$\mathcal{B}(\bar{B}^0 \to D^0\bar{K}^{*0}) = (4.0 \pm 0.7 \pm 0.3) \times 10^{-5}$$
$$\mathcal{B}(\bar{B}^0 \to \bar{D}^0\bar{K}^{*0}) = (0.0 \pm 0.5 \pm 0.3) \times 10^{-5}$$

where the uncertainties are, respectively, statistical and systematic. For the decay $\bar{B}^0 \to \bar{D}^0\bar{K}^{*0}$ we use the Bayesian method to compute the upper limit N_{UL} on the observed number of events. The value of N_{UL} at 90% C.L. is defined as $\int_0^{N_{\mathrm{UL}}} \mathcal{L}(N)dN = 0.9$, where $\mathcal{L}(N)$ is the likelihood function from the fit to the m_{ES} and ΔE distributions. We assume a flat prior probability density function for $\mathcal{B} > 0$. We account for systematic uncertainties by numerically convolving $\mathcal{L}(N)$ with a Gaussian distribution with a width determined by the relative systematic uncertainty multiplied by the measured signal yield. We obtain $\mathcal{B}(\bar{B}^0 \to \bar{D}^0\bar{K}^{*0}) < 1.1 \times 10^{-5}$ at 90% C.L.

We compute an upper limit on the ratio $\tilde{r}_B$ by measuring the ratio $\mathcal{R}_i$ in each D^0 decay mode. We use the expression $\mathcal{R}_i = (\varepsilon_{D_i\bar{K}}/\varepsilon_{\bar{D}_i\bar{K}}) \cdot (N_{\bar{D}_i\bar{K}}/N_{D_i\bar{K}})$ to obtain the PDF for $\mathcal{R}_i$ from the unbinned maximum likelihood fit described earlier. In this expression $\varepsilon_{\bar{D}_i\bar{K}}$ ($\varepsilon_{D_i\bar{K}}$) and $N_{\bar{D}_i\bar{K}}$ ($N_{D_i\bar{K}}$) are, respectively, the reconstruction efficiency and fitted yield of the $\bar{B}^0 \to \bar{D}^0\bar{K}^{*0}$, $\bar{D}^0 \to K^-X_i^+$ ($\bar{B}^0 \to D^0\bar{K}^{*0}$, $D^0 \to K^-X_i^+$) decay modes. The uncertainties on $\varepsilon_{\bar{D}_i\bar{K}}$, $\varepsilon_{D_i\bar{K}}$, and $N_{D_i\bar{K}}$ are used to obtain the posterior PDF $\mathcal{L}(\mathcal{R}_i)$ for each $\mathcal{R}_i$. We assume a Gaussian PDF for r_{D_i}. We compute the PDF for $\tilde{r}_B$ by convolving $\mathcal{L}(\mathcal{R}_i)$ and r_{D_i} according to Eq. (1). We obtain the limit $\tilde{r}_B < 0.40$ at 90% C.L. with a Bayesian method using uniform priors for $\mathcal{R}_i > 0$ and by taking into account the full range $0°–180°$ for γ and δ_i. The present signal yields combined with this limit on $\tilde{r}_B$ suggest that a substantially larger data sample is needed for a competitive time-dependent measurement of $\sin(2\beta + \gamma)$ in $\tilde{B}^0 \to D^{(*)0}\tilde{K}^0$ decays.

In summary, we have presented measurements of the branching fractions for the decays $\tilde{B}^0 \to D^0\tilde{K}^0$ and $\bar{B}^0 \to D^0\bar{K}^{*0}$, evidence for the decay $\tilde{B}^0 \to D^{*0}\tilde{K}^0$, and an upper limit for the ratio $\tilde{r}_B$. Our results are in agreement with previous measurements of these modes [18].

[1] B. Aubert *et al.* (*BABAR* Collaboration), Phys. Rev. Lett. **87**, 091801 (2001); K. Abe *et al.* (Belle Collaboration), Phys. Rev. Lett. **87**, 091802 (2001).

[2] B. Aubert *et al.* (*BABAR* Collaboration), Phys. Rev. Lett. **94**, 161803 (2005); K. Abe *et al.* (Belle Collaboration), Phys. Rev. D **71**, 072003 (2005).

[3] N. Cabibbo, Phys. Rev. Lett. **10**, 531 (1963); M. Kobayashi and T. Maskawa, Prog. Theor. Phys. **49**, 652 (1973).

[4] K. Abe, Proceedings of the XXII International Symposium on Lepton-Photon Interactions at High Energy, Uppsala, Sweden, 2005 (to be published).

[5] M. Gronau and D. London, Phys. Lett. B **253**, 483 (1991); D. Atwood, I. Dunietz, and A. Soni, Phys. Rev. Lett. **78**, 3257 (1997); B. Kayser and D. London, Phys. Rev. D **61**, 116013 (2000); A. I. Sanda, hep-ph/0108031.

[6] Charge conjugation is implied throughout this paper, unless explicitly stated otherwise.

[7] T. E. Coan *et al.* (CLEO Collaboration), Phys. Rev. Lett. **88**, 062001 (2002); K. Abe *et al.* (Belle Collaboration), Phys. Rev. Lett. **88**, 052002 (2002); B. Aubert *et al.* (*BABAR* Collaboration), Phys. Rev. D **69**, 032004 (2004).

[8] P. Krokovny *et al.* (Belle Collaboration), Phys. Rev. Lett. **90**, 141802 (2003).

[9] S. Eidelman *et al.* (Particle Data Group), Phys. Lett. B **592**, 1 (2004).

[10] B. Aubert *et al.* (*BABAR* Collaboration), Nucl. Instr. Meth., Sect. C A **479**, 1 (2002).

[11] S. Agostinelli *et al.* (GEANT4 Collaboration), Nucl. Instr. Meth., Sect. C A **560**, 250 (2003).

[12] D. J. Lange, Nucl. Instrum. Methods Phys. Res., Sect. A **462**, 152 (2001).

[13] S. Kopp *et al.* (CLEO Collaboration), Phys. Rev. D **63**, 092001 (2001).

[14] R. A. Fisher, Annals Eugen. **7**, 179 (1936).

[15] E. Farhi, Phys. Rev. Lett. **39**, 1587 (1977).

[16] H. Albrecht *et al.* (ARGUS Collaboration), Z. Phys. C **48**, 543 (1990).

[17] The contribution of misreconstructed B background in the $\bar{B}^0 \to \bar{D}^0 \bar{K}^{*0}$ mode, where no signal is observed, is about two events.

[18] K. Abe *et al.* (Belle Collaboration), hep-ex/0408108.